2. Makio Shozu, Takashi ehara, Akira Mitsuhashi. Metformin, An Old Drug for a New Endocrine Therapy to Endometrial Cancer. 15th International Congress on Hormonal Steroids and Hormones & Cancer. 2012年11月15日～17日、Kanazawa
3. 生水真紀夫. 胎盤におけるアロマターゼ発現と性差構築. 第4回文部科学省科学研究費補助金新学術領域研究「性差構築の分子基盤」領域会議. 2012年10月15日～17日、和歌山
4. 生水真紀夫. アロマターゼの進化：なぜ胎盤で発現したか？. 東京医科歯科大学大学院特別講義. 2012年5月18日、東京
5. 生水真紀夫. エストロゲンと骨－思春期症例から学ぶ. 岐阜産科婦人科研究会. 2012年8月25日、岐阜
6. 生水真紀夫. 女性のライフサイクルとエストロゲン－アロマターゼとのかかわり－. 第27回日本女性医学学会学術集会. 2012年10月13日、山形
7. 生水真紀夫. 骨とエストロゲン－思春期の症例に学ぶ－. 埼玉県産婦人科医会平成24年度後期学術集会. 2012年11月10日、埼玉

H. 知的財産権の出願・登録状況

1. 特許取得

なし

2. 実用新案登録

なし

3. その他

なし

厚生労働科学研究費補助金 難治性疾患等克服研究事業（難治性疾患克服研究事業）

分担研究報告書

遺伝性女性化乳房の分子遺伝学的診断法の開発と評価

研究分担者　深見真紀　　国立成育医療研究センター研究所　部長

研究要旨

遺伝性女性化乳房症の臨床検体を解析し、下記の点を明らかとした。(1) 本症の原因となるアロマターゼ遺伝子周辺のゲノム構造異常の形成には、DNA複製時のエラーと組み換え異常の両者が関与する。(2) 遺伝性女性化乳房症におけるアロマターゼ過剰発現の原因は、アロマターゼプロモーターもしくは翻訳領域のコピー数増加、および、広範囲発現性隣接遺伝子プロモーターの獲得である。(3) これらの異常の同定には、アレイ comparative genomic hybridization (CGH) がきわめて有用である。一方、アレイCGHで異常が同定されない症例が存在することから、本症の発症に未知の要因が関与する可能性が示唆される。(4) 乳がんの発症には、アロマターゼ遺伝子周辺コピー数異常の関与は少ないと推測される。

他の厚生労働省研究班との連携

本研究は、厚生労働省　難病・がん等の疾患分野の医療の実用化事業（小児科・産科領域の大規模遺伝子配列解析による病因解明とゲノム解析拠点整備）および難治性疾患克服研究事業（性分化疾患の実態把握と病態解明ならびに標準的診断・治療指針の作成）と連携して研究を推進した。

A．研究目的

遺伝性女性化乳房は、思春期からの乳房腫大および性腺機能障害などにより長期のQOL低下を招く難治疾患である。本研究の目的は、遺伝性女性化乳房患者の分子遺伝学的解析により、本症の発症機序を解明し、診断法を開発することである。

B．研究方法

1.　遺伝性女性化乳房患者におけるゲノム構造異常の同定

臨床的に遺伝性女性化乳房と診断された10家系を対象として、本研究班で独自に開発したカスタムアレイ comparative genomic hybridization (CGH) を用いてアロマターゼ遺伝子 (*CYP19A1*) 周辺領域のゲノムコピー数解析を行った。異常が同定された患者では、可能な限り切断点の塩基配列を決定し、ゲノム構造を明確にした。得られた塩基配列はNCBI BLAST Search (http://blast.ncbi.nlm.nih.gov/) で解析した。CGH で異常が同定されなかった症例に関しては、エストロゲン受容体α、β遺伝子のシークエンスを行った。

2.　乳がん組織における *CYP19A1* 周辺領域ゲノム構造異常の解析

乳がん患者のがん組織42からゲノムDNAを抽出し、カスタムアレイ CGH を用いて *CYP19A1* 周辺領域のコピー数解析を行った。42例中5例はESR陰性、他は陽性であった。

（倫理面への配慮）

本研究は、ヒトゲノム・遺伝子解析研究に関する倫理指針（平成16年文部科学省・厚生労働省・経済産業省告示第1号）を遵守して施行した。

本研究課題は、国立成育医療研究センターおよび千葉大学・大阪大学の倫理委員会において承認されている。臨床検体は、患者本人または両親から書面でのインフォームドコンセントを得たのちに採取した。検体は、各医療機関で個人識別情報をなくして匿名化された後に当研究機関に送付された。

C．研究結果

1. 遺伝性女性化乳房患者におけるゲノム構造異常の同定

新規患者を含む12家系で*CYP19A1*過剰発現を招く15q21領域のコピー数異常を同定し、そのゲノム構造を解明した。その結果、遺伝性女性化乳房の発症に15q21領域の微小欠失と重複のほか、複数の切断点を有する複雑構造異常が関与することが明確となった（図1）。

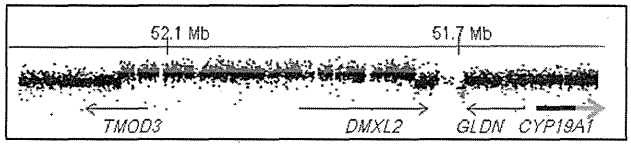

これらの微細構造異常の成立には、組み換え異常に起因するnon-homologous end joining（NHEJ）とnon-allelic recombination（NAHR）のみならず、DNA複製エラーに起因するFork stalling and template switching（FoSTeS）が関与すると推測される。このことから、*CYP19A1*周辺領域にゲノム脆弱性を招くモチーフが存在することが示唆される。また、本症の発症には、アロマターゼプロモーターもしくは翻訳領域のコピー数増加、および、広範囲に発現する6つの隣接遺伝子プロモーターと*CYP19A1*翻訳領域のキメラ遺伝子形成が関与することが明らかとなった（図2）。

患者のCGH解析により、微小欠失、微小重複、複雑構造異常が同定可能であった。とくに、これまで単純な染色体逆位と考えられていた2家系においても、複雑構造異常が同定された。一方、今回臨床的に診断された10家系のうち、4家系では明らかなゲノム異常が同定されなかった。さらに、これらの家系では、エストロゲン受容体α、β遺伝子に変異は同定されなかった。

2. 乳がん組織におけるCYP19A1周辺領域ゲノム構造異常の解析

乳がん組織42例では*CYP19A1*周辺領域コピー数異常は同定されなかった。

D．考察

1. 遺伝性女性化乳房症の原因

本症の発症に、DNA複製エラーと組み換え異常の両者が関与することか明確となった。このような異常により*CYP19A1*のプロモーターもしくは翻訳領域のコピー数増加、および、隣接遺伝子と*CYP19A1*からなるキメラ遺伝子が生じ、*CYP19A1*過剰発現を招くと推測される。患者の重症度は、当該患者における獲得プロモーターの機能を反映すると推測される。

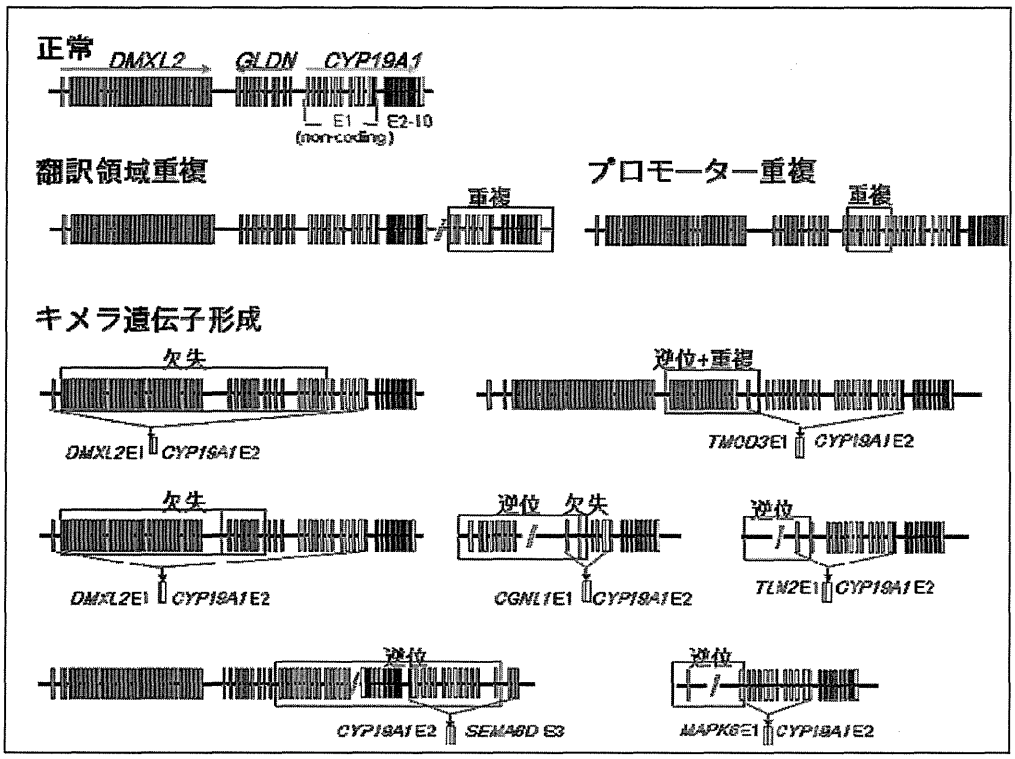

2. 遺伝性女性化乳房症の診断

本症の診断には、カスタムアレイCGH解析がきわめて有用であることが明確となった。一方、CGHで異常が同定されない症例が存在することから、本症の発症には未知の要因が関与する可能性がある。今後、変異陰性家系のエクソーム解析や全ゲノムコピー数解析などにより、新規発症機序が解明されると期待される。

3. 乳がん組織における *CYP19A1* 周辺領域ゲノム構造異常

本研究によって、乳がん発症における 15q21 領域の欠失/重複の関与は少ないことが見出された。したがって、体細胞における *CYP19A1* 周辺領域の新規ゲノム異常の形成は少ないと推測される。この結果とこれまでの研究成果を統合すると、乳がん組織におけるアロマターゼ過剰発現には、ゲノム構造異常ではなくサイトカインによる *CYP19A1* プロモータースイッチの関与が大きいことが示唆される。

E. 結論

遺伝性女性化乳房症の原因となるゲノム微細構造異常とその成立メカニズムを明確とした。また、このような異常の同定に、カスタムアレイ CGH が有用であることを見出した。一方、本症の発症には、未知の要因が関与する可能性が見出された。また、乳がんの発症には、*CYP19A1* 周辺領域コピー数異常の関与が少ないことがあきらかとなった。

F. 健康危険情報

なし

G. 研究発表

1. 論文発表

1. Fukami M, Shozu M. Ogata T. Molecular Bases and Phenotypic Determinants of Aromatase Excess Syndrome. Int J Endocrinol. 584807.2012
2. 深見真紀，曽根田瞬，加藤芙弥子，花木啓一，神埼晋，大山建司，佐野友昭，西垣敏紀，稲垣朱実，高木博史，Gerhard Binder，横谷進，堀川玲子，生水真紀夫，緒方勤.アロマターゼ過剰症 6 家系の分子遺伝学的/臨床的解析：新たな遺伝疾患発症機序とホルモン調節機構の解明.ホルモンと臨床.特集小児内分泌学の進歩 2011. 59: 27-32, 2012

2. 学会発表・講演会

1. 深見真紀.小児内分泌疾患診療に役立つ分子遺伝学の知識. 獨協医科大学越谷病院小児科セミナー. 2012 年 2 月 13 日，越谷
2. 深見真紀.アロマターゼ過剰症とゴナドトロピン分泌. 日本内分泌学会シンポジウム. 2012 年 4 月 26 日，名古屋
3. 深見真紀，五十嵐麻希，阿部修司，山本幸代，金城さおり，緒方勤.男性における乳房腫大（女性化乳房）. 第 46 回小児内分泌学会 とっておきの症例. 2012 年 9 月 27～29 日，大阪

H. 知的財産権の出願・登録状況

1. 特許取得

なし

2. 実用新案登録

なし

3. その他

なし

厚生労働科学研究費補助金 難治性疾患等克服研究事業（難治性疾患克服研究事業）

分担研究報告書

遺伝性女性化乳房症例に関する文献調査

研究分担者　碓井宏和　　千葉大学大学院医学研究院生殖医学　講師
花木啓一　　鳥取大学医学部保健学科母性・小児家族看護学・小児保健学　教授
野口眞三郎　　大阪大学大学院医学系研究科乳腺内分泌外科　教授

研究要旨

1983年から2012年の間に医学文献データベース医学中央雑誌に収載された国内文献の調査を実施した。その結果、661件のヒットがあり、重複例などを除き341件の女性化乳房症例の報告があった。女性化乳房症の原因を文献記載から分類したところ、63症例が原因不明、すなわち特発性女性化乳房症と考えられた。

特発性症例63例のうち6症例に家族歴の記載があり、遺伝性女性化乳房症の症例である可能性が高いと考えられた。実際に、うち3症例では、アロマターゼ過剰症であったと報告されている。特発例の診断は小児科で行われている例が多く、特に遺伝性女性化乳房症と考えられた6症例のうち4例は小児科、2例は内科からの報告であった。

この2年間に、細胞遺伝学的にアロマターゼ過剰症と診断された症例・総説が本研究班の班員から報告されており、世界中の遺伝性女性化乳房症患者の半数以上がわが国からの報告であった。確定診断例が徐々に増加しているが、現時点では発症前診断例は皆無であった。

A．研究目的

遺伝性女性化乳房症は、思春期前の男性に女性化乳房、低身長・性欲の低下、さらには精神的問題から社会的活動性の低下をきたす疾患である。伴性劣性遺伝形式と考えられた症例も過去には報告されているものの、最近の報告は常染色体優性遺伝形式の症例がほとんどである。したがって、女性にも発症し、この場合には思春期早発症・巨大乳房・不正性器出血などの症状をきたす。

本症の疾患概念は、医療者にもあまり認知されておらず、本症を専門とする診療科もない。

2010年に遺伝性女性化乳房症の実態把握のためのアンケート調査を施行したが、2010年以降も、われわれは本邦における本疾患患者を調査し、臨床像や診療の現状の把握に努めてきた。本年度は、これらの基礎的データをもとに診断基準案を作成した。

本研究では、文献調査を継続し、アンケート実施以降に変化が生じたか検証した。同時に、本邦における遺伝性女性化乳房症の現状・問題点を確認した。

B．研究方法

医学文献データベース医学中央雑誌を用いて国内症例の文献調査を行った。1983年から2012年までに報告された女性化乳房症例の報告（検索語: 女性化乳房/TH or 女性化乳房/AL）を検索し、タイトル・抄録を基に女性化乳房症例を分類・集計した。

さらに、英文文献での報告症例の調査も継続して実施した。PubMedを用い、(gynecomastia) AND (familiar or hereditary)、(Aromatase excess syndrome)をキーワードとして検索し、ヒットした文献について個別に調査し、本症に該当する症例であるか否かを検討した。

（倫理面への配慮）
特になし。

C．研究結果

2010年度より開始した調査を継続し、2010年以降に追加報告された症例がないか文献調査を実施

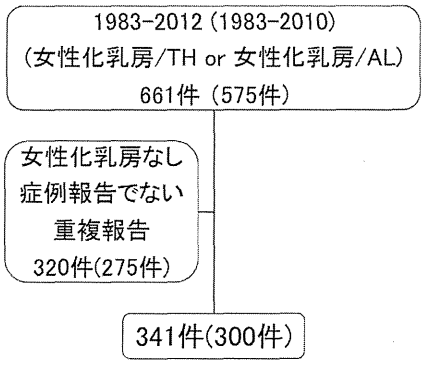

図1 医学中央雑誌“女性化乳房”

表1 文献で推定されていた女性化乳房の原因

薬剤	31	薬剤性	31
先天性	41	染色体異常	25
		酵素欠損症	4
		アンドロゲン受容体関連	12
神経筋疾患	44	神経筋疾患	44
腫瘍	102	腫瘍	76
		男性乳癌	26
ホルモン	31	高プロラクチン血症	6
		甲状腺疾患	10
		中枢性ホルモン異常	15
その他	29	透析	10
		肝硬変	6
		その他	13
特発性疑い	63	特発性疑い	63

した。機械検索の後、タイトル・抄録を実際に確認し、女性化乳房と無関係のもの、症例報告ではないもの、さらに重複報告と思われるものを除外したところ、女性化乳房症例の報告は計 341 件（41 件追加）となった（図１）。341 例のそれぞれについて、推定されていた女性化乳房の原因は、2010 年調査時と大きい変化はなかった（表１）。

特発性女性化乳房症疑い例の中で、家族歴を有する、すなわち遺伝性女性化乳房症家系が、最近２年間で３家系が追加された。３家系ともにアロマターゼ過剰症であったと報告されている。うち２家系は本研究班員からの報告であった。

表2 診療科別女性化乳房症報告数

	女性化乳房症	特発性疑い例	（家族性）
内科	79	3	(2)
外科	70	22	
神経内科	44	0	
小児	33	14	(4)
呼吸器	29	0	
泌尿器	27	0	
形成	18	9	
皮膚	17	4	
小児外	6	2	
放射線	3	0	
精神	2	0	
婦人	1	1	
その他・不明	12	3	

遺伝性女性化乳房症と考えられた6症例のうち4例は小児科、2例は内科からの報告であり、本疾患が、前思春期から顕在化してくることに符合している（表２）。この２年間に、アロマターゼ過剰症の総説が本研究班の班員から４編報告されている。

欧文文献についても調査を実施したが、最近 2 年間の新規報告例は、本研究班からの報告だけであった。

D．考察

これまでは、細胞遺伝学的にアロマターゼ過剰症の診断がついた報告はほとんどなかったが、最近報告された３家系は、いずれも、アロマターゼ過剰症が原因であったと報告されている。2010 年に、われわれの実施した遺伝性女性化乳房症の実態把握のためのアンケート調査は、全国の医育機関・研修指定病院を中心とする基幹施設を対象とし、乳腺外科領域（日本乳癌学会認定・関連施設）、形成外科領域（認定・教育関連施設）、小児科領域（小児内分泌学会会員）、内科領域（日本内分泌学会 認定教育施設）と当該疾患患者が受診する可能性の高い施設がほぼ網羅されていた。アンケート調査により、疾患の認知度が上昇し、確定診断に至る症例が増えてきた可能性がある。

班員の深見らの報告では、9 家系 23 例の男性遺伝性アロマターゼ過剰症の詳細が報告されている（Int J Endocrinol. 2012:584807, J Clin Endocrinol Metab. 2011;96:E1035-43）。1977 年以降に欧文で発表された本症と思われる症例の約半数を占めている。

遺伝性女性化乳房症の女児例は、兄が発端者となった兄妹例以外では、現時点では報告がない。また前述の深見らの報告において、発端者の両親に対して保因者診断が行われた症例に着目すると、父親が遺伝性女性化乳房症であった症例が 1 例であったのに対して、母親が保因者であった症例は 4 例であった。遺伝性女性化乳房症は思春期前の時期から

アロマターゼ阻害剤を投与することにより思春期早発、女性化乳房、低身長などの発症を予防することができると考えられるが、保因者が母親であった場合は、母親自身が、アロマターゼ過剰症であることに気がつくことは難しいため、子どもがアロマターゼ過剰症であったとしても、発症する前の早期診断は現時点では困難と考えられる。アロマターゼ過剰症患児の早期発見法の開発が次なる課題と考えられる。

E. 結論

1983年から2012年の本邦文献では、63名の特発性女性化乳房症の患者が報告されていた。確定診断されている症例が徐々に増えつつある。一方、発症前診断は現時点では1例も行われていなかった。

F. 健康危険情報

なし

G. 研究発表

1. 論文発表

1. Furuya M, Okuda M, Usui H, Takenouchi T, Kami D, Nozawa A, Shozu M, Umezawa , Takahashi T, Aoki. Expression of Angiotensin II receptor-like 1 (APJ) in the Placentas of Pregnancy-Induced Hypertension. Int J Gynecol Pathol 2012; 31(3): 227-35
2. Kizaki Shoko, Matsui Hideo, Usui Hirokazu, Shozu Makio, Hanawa Shinsuke, Yamamoto Eiko, and Kikkawa Fumitaka. Normal human Chorionic Gonadotropin Regression Curves in Uneventful Postmolar Patients. J Reprod Med.2012; 57(5-6): 243-248
3. Kihara Maki, Usui Hirokazu, Tanaka Hirokazu, Inoue Hiromi, Matsui Hideo, Shozu Makio. Complicating Preeclampsia as a Predictor of Poor Survival of the Fetus in complete Hydatidiform Mole Coexistent with Twin Fetus. J Reprod Med.2012; 57(7-8): 325-328
4. Mitsuhashi A, Uno T, Usui H, Nishikimi K, Yamamoto N, Watanabe M, Tate S, Hirashiki K, Kato K, Yamazawa K, Shozu M. Daily Low-Dose Cisplatin-Based Concurrent Chemoradiotherapy in Patients With Uterine Cervical Cancer With Emphasis on Elderly Patients: A Phase 2 Trial. Int J Gynecol Cancer.2012;
5. 碓井宏和. 腫瘍　症例に学ぶ　非順調型の臨床経過を辿る絨毛性疾患　低単位hCGの取扱いについて. 日本産科婦人科学会雑誌. 64 (9) N-290-N-294
6. 木村定雄、西山眞理子、碓井宏和. 閉経後高血圧の新しい発症経路の解明　血管平滑筋AT1受容体・RGS・SPLの相互作用解析. 大和証券ヘルス財団研究業績集2012 ; (35) : 31-35

2. 学会発表・講演会

1. Hirokazu Usui. The polymorphisms of folate metabolic enzyme gene and gestational trophoblastic disease. International Federation of Placenta Associations Meeting 2012. 2012年9月18日～20日、広島
2. 碓井宏和. 特別講演「最近の絨毛性疾患の取扱い」. 第52回東総産婦人科医会講演会. 2012年3月2日（旭）
3. 碓井宏和. 症例に学ぶ　非順調型の臨床経過を辿る絨毛性疾患　低単位hCGの取扱いについて. 第64回日本産科婦人科学会学術講演会. 2012年4月13日～15日、神戸
4. 碓井宏和. 婦人科悪性腫瘍と妊孕能温存　その2絨毛性疾患. 第53回特定非営利活動法人日本婦人科腫瘍学会学術講演会. 2012年11月23日、岡山

H. 知的財産権の出願・登録状況

1. 特許取得

なし

2. 実用新案登録

なし

3. その他

なし

Ⅲ. 研究成果の刊行一覧・別刷

研究成果の刊行に関する一覧表

雑誌

発表者氏名	論文タイトル名	発表誌名	巻号	ページ	出版年
Maki Fukami, Junichi Suzuki, Kazuhiko Nakabayashi, Ryo Tsunashima, Tsutomu Ogata, Makio Shozu, Sinzaburo Noguchi	Lack of genomic rearrangements involving the aromatase gene *CYP19A1* in breast cancer	Breast Cancer	2013	Published online (4 pages)	2013
Fukami M, Shozu M, Ogata T	Molecular Bases and Phenotypic Determinants of Aromatase Excess Syndrome	Int J Endocrinol.	2012	584807	2012
深見真紀，曽根田瞬，加藤芙弥子，花木啓一，神埼晋，大山建司，佐野友昭，西垣敏紀，稲垣朱実，高木博史，Gerhard Binder，横谷進，堀川玲子，生水真紀夫，緒方勤	アロマターゼ過剰症６家系の分子遺伝学的/臨床的解析：新たな遺伝疾患発症機序とホルモン調節機構の解明	ホルモンと臨床	59	27-32	2012

Breast Cancer
DOI 10.1007/s12282-013-0471-5

RAPID COMMUNICATION

Lack of genomic rearrangements involving the aromatase gene *CYP19A1* in breast cancer

Maki Fukami · Junichi Suzuki · Kazuhiko Nakabayashi · Ryo Tsunashima · Tsutomu Ogata · Makio Shozu · Shinzaburo Noguchi

Received: 25 February 2013 / Accepted: 15 April 2013

Abstract Increased intratumoral expression of aromatase, the key enzyme for estrogen biosynthesis, is predicted to be of critical importance in the development of breast cancer. Recently, several germline rearrangements at 15q21 have been shown to cause overexpression of the aromatase gene *CYP19A1* and resulting aromatase excess syndrome. To determine whether submicroscopic genomic rearrangements at 15q21 are involved in aromatase overexpression in breast cancer tissues, we investigated copy-number alterations in genomic DNA obtained from 44 tumor samples. Comparative genomic hybridization analysis identified no deletion or duplication at 15q21 in the 44 samples. These results, in conjunction with previous data, indicate that aromatase overexpression in breast cancer tissues is likely to result from a promoter switch of *CYP19A1* and/or accumulation of *CYP19A1*-expressing cells, rather than from cryptic transactivation of *CYP19A1* because of genomic rearrangements at 15q21.

Keywords Breast cancer · Aromatase · *CYP19A1* · Gene expression · Genomic rearrangement

Abbreviations
AEXS Aromatase excess syndrome
CGH Comparative genomic hybridization

Introduction

Estrogens stimulate the proliferation of breast cancer cells, possibly by transactivating growth factor genes or oncogenes [1, 2]. Although estrogens are usually synthesized in a variety of tissues, including ovaries, skin, and fat, they can also be produced locally in breast cancer tissues [1, 3, 4]. Previous studies have revealed enhanced expression of aromatase, the key enzyme for estrogen biosynthesis, in breast cancer epithelial cells and in immature fibroblasts around the malignant cells [1, 4, 5]. Aromatase overexpression in breast cancer tissues is predicted to be critically important in tumor development [1, 5].

Recently, we and other groups have described an autosomal dominant disorder referred to as aromatase excess syndrome (AEXS), which is characterized by gynecomastia resulting from increased expression of the aromatase gene *CYP19A1* [6–8]. The molecular bases of AEXS include tandem duplications at 15q21.2 involving the promoter region of *CYP19A1* and a variety of deletions and

M. Fukami (✉) · J. Suzuki · T. Ogata
Department of Molecular Endocrinology, National Research Institute for Child Health and Development, 2-10-1 Okura, Setagaya, Tokyo 157-8535, Japan
e-mail: fukami-m@ncchd.go.jp

J. Suzuki
Department of Pediatrics and Child Health, Nihon University School of Medicine, Tokyo, Japan

K. Nakabayashi
Department of Maternal-Fetal Biology, National Research Institute for Child Health and Development, Tokyo, Japan

R. Tsunashima · S. Noguchi
Department of Breast and Endocrine Surgery, Osaka University Graduate School of Medicine, Osaka, Japan

T. Ogata
Department of Pediatrics, Hamamatsu University School of Medicine, Hamamatsu, Japan

M. Shozu
Department of Reproductive Medicine, Graduate School of Medicine, Chiba University, Chiba, Japan

Published online: 30 April 2013

Table 1 Breast cancer samples examined in this study

Sample	ER[a]	PR[a]	HER2[b]	Menopausal status	Age (years)
1	Positive	Positive	Negative	Postmenopausal	78
2	Positive	Positive	Negative	Postmenopausal	63
3	Positive	Positive	Negative	Postmenopausal	51
4	Positive	Positive	Negative	Postmenopausal	56
5	Positive	Positive	Negative	Postmenopausal	55
6	Positive	Positive	Negative	Postmenopausal	65
7	Positive	Positive	Negative	Postmenopausal	58
8	Positive	Positive	Negative	Postmenopausal	71
9	Positive	Positive	Negative	Postmenopausal	64
10	Positive	Positive	Negative	Postmenopausal	66
11	Positive	Positive	Negative	Postmenopausal	59
12	Positive	Positive	Negative	Postmenopausal	81
13	Positive	Positive	Negative	Postmenopausal	61
14	Positive	Positive	Negative	Postmenopausal	68
15	Positive	Positive	Negative	Postmenopausal	65
16	Negative	Negative	Negative	Postmenopausal	67
17	Negative	Negative	Negative	Premenopausal	49
18	Negative	Negative	Positive	Postmenopausal	68
19	Negative	Negative	Negative	Postmenopausal	70
20	Negative	Negative	Positive	Premenopausal	42
21	Positive	Positive	Negative	Postmenopausal	73
22	Positive	Positive	Negative	Postmenopausal	56
23	Positive	Positive	Negative	Postmenopausal	56
24	Positive	Positive	Negative	Postmenopausal	57
25	Positive	Positive	Negative	Postmenopausal	56
26	Positive	Positive	Negative	Postmenopausal	70
27	Positive	Positive	Negative	Postmenopausal	71
28	Positive	Positive	Negative	Postmenopausal	80
29	Positive	Positive	Negative	Postmenopausal	60
30	Positive	Positive	Negative	Postmenopausal	80
31	Positive	Positive	Negative	Postmenopausal	72
32	Positive	Positive	Negative	Postmenopausal	64
33	Positive	Positive	Negative	Postmenopausal	65
34	Positive	Positive	Negative	Postmenopausal	80
35	Positive	Positive	Negative	Postmenopausal	59
36	Positive	Positive	Negative	Postmenopausal	60
37	Positive	Positive	Negative	Postmenopausal	62
38	Positive	Positive	Negative	Postmenopausal	63
39	Positive	Positive	Negative	Postmenopausal	58
40	Positive	Positive	Negative	Postmenopausal	69
41	Positive	Positive	Negative	Postmenopausal	65
42	Positive	Positive	Negative	Postmenopausal	70
43	Positive	Positive	Negative	Postmenopausal	62
44	Positive	Positive	Negative	Postmenopausal	69

ER estrogen receptor; *PR* progesterone receptor; *HER2* human epidermal growth factor receptor 2

[a] ER and PR were analyzed by use of immunohistochemical assays. The results were defined as positive when more than 10 % of the tumor cells were positively stained

[b] HER2 amplification was analyzed by fluorescence in situ hybridization analysis. Signal intensities >2.0 were assessed as positive

inversions at 15q21.1-21.3 that create chimeric genes consisting of coding exons of *CYP19A1* and the promoter-associated exons of other genes. Identification of highly heterogeneous rearrangements in patients with AEXS indicates that the chromosomal region around *CYP19A1* is particularly vulnerable to genomic abnormalities [8]. Therefore, submicroscopic rearrangements at 15q21 generated in germ cells or in somatic cells may underlie

aromatase overexpression in breast cancer tissues. Here, we performed copy-number analysis of the 15q21 region in 44 genomic DNA samples obtained from breast cancer tissues.

Materials and methods

Tumor tissue samples

This study was approved by the Institutional Review Board Committees at Osaka University and the National Center for Child Health and Development. After obtaining written informed consent, breast cancer tissues were obtained at surgery from 44 Japanese females aged 42–80 years (Table 1). The samples were frozen in liquid nitrogen. All 44 tumors were invasive ductal carcinoma. The samples were examined for levels of expression of estrogen receptor and progesterone receptor, and for amplification of human epidermal growth factor receptor 2, as described elsewhere [9] (Table 1).

Comparative genomic hybridization analysis

Genomic DNA was extracted from tumor tissues by use of a DNeasy blood and tissue kit (Qiagen, Maryland, USA). The DNA samples were subjected to comparative genomic hybridization (CGH) analyses by use of a custom-made oligoarray (8 × 60 k format; Agilent Technologies, Palo Alto, CA, USA). The array contained approximately 16,000 probes for the 1.5 Mb region at 15q21 (chr15:51,000,000–52,500,000; hg 19, build 37), together with several reference probes for other genomic regions. The procedure was conducted in accordance with the manufacturer's instructions. A genomic DNA sample obtained from leukocytes of an unaffected Japanese 58-year-old female was used as a control.

Results

CGH analysis

Comparative genomic hybridization analysis indicated a normal copy-number for exons 1–10 of *CYP19A1* in the 44 samples (Fig. 1a). Furthermore, no deletion or duplication was detected in the 1.5 Mb genomic region at 15q21 (Fig. 1a).

Discussion

Comparative genomic hybridization analysis identified no copy-number alterations at 15q21 in 44 breast cancer tissues. It is worth remarking that the method used in this

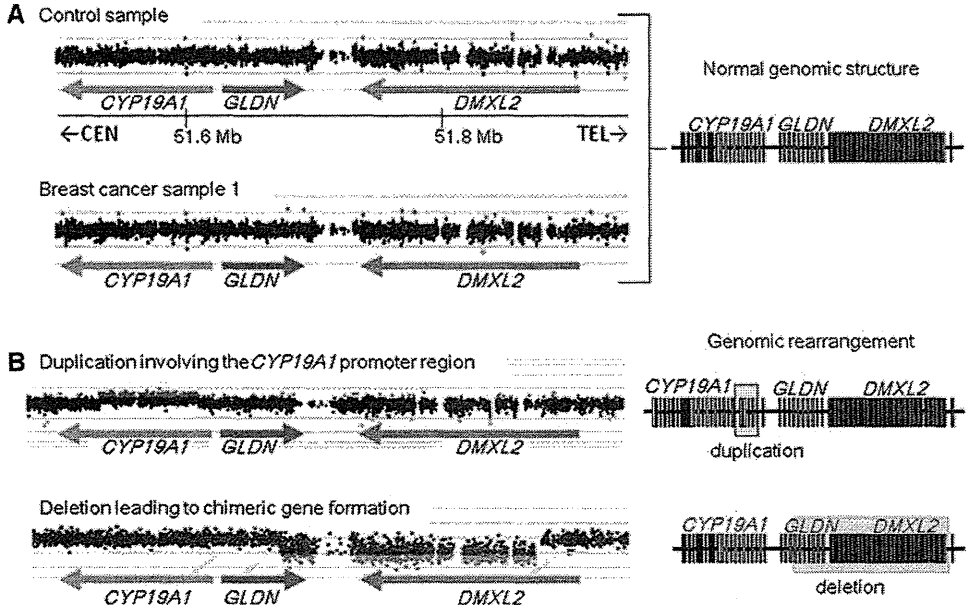

Fig. 1 **a** Comparative genomic hybridization (CGH) analysis (*left panel*) and schematic representation of the normal genomic structure in the control and breast cancer samples (*right panel*). The *black*, *red*, and *green dots* denote signals indicative of normal, increased (>+0.5), and reduced (<−1.0) copy-numbers, respectively. The *arrows* indicate genomic positions of *CYP19A1*, *GLDN*, and *DMXL2* (5′ → 3′). The positions correspond to the human genome reference assembly (UCSC genome browser, February 2009, hg19, build 37). **b** Genomic abnormalities previously identified in patients with aromatase excess syndrome. These germline rearrangements have been implicated in *CYP19A1* overexpression [8]. The results of CGH analysis (*left panel*) and schematic representation of the rearranged genome (*right panel*) are shown

study is capable of identifying all the duplications and deletions that have previously been associated with AEXS (Fig. 1b) [8], although copy-number-neutral inversions may not be detected by CGH analysis. These results imply that copy-number gains of *CYP19A1* and formation of chimeric genes arising from cryptic rearrangements are not the major factors underlying aromatase overexpression in breast cancer tissues. Furthermore, lack of genomic rearrangements in the 15q21 region in the 44 samples suggests that this region would not be a hotspot for somatic rearrangements, especially considering that breast cancer tissues are characterized by prominent genomic instability [10].

Previous studies have attributed aromatase overexpression in breast cancer tissues to alternative use of the non-coding exons 1 of *CYP19A1* [5, 11]. Of the 11 exons 1, exons 1.3, II, and 1.7 were found to predominantly control expression of *CYP19A1* in breast cancer tissues, whereas exon 1.4 functioned as the major promoter in normal breast tissues. This promoter switch seemed to result from the perturbed production of signal molecules in tumor tissues. For example, overproduction of prostaglandins has been associated with activation of exons 1.3 and II [1, 5, 11]. Furthermore, accumulation of immature adipose fibroblasts with strong expression of *CYP19A1* has also been proposed to contribute to aromatase excess in breast cancer tissues [5].

It should be noted that our conclusion is based on results from 44 samples only. Furthermore, *CYP19A1* mRNA levels were not analyzed in this study. In this regard, it is known that although increased aromatase activity is a common feature in breast cancer tissues, mRNA levels of *CYP19A1* vary among samples [12, 13]. Therefore, the absence of genomic rearrangements in our 44 samples may be ascribed to low expression of *CYP19A1* in these tissues. Indeed, genomic rearrangements at 15q21 may be hidden in a specific group of breast cancers with overexpression of *CYP19A1*. Further CGH and mRNA analysis for several tumor samples is necessary to clarify the presence or absence of an association between genomic rearrangements at 15q21 and intratumoral estrogen overproduction.

In summary, this study, in conjunction with previous data, implies that aromatase overexpression in breast cancer tissues is likely to result from a promoter switch of *CYP19A1* induced by trans-acting factors and/or accumulation of *CYP19A1*-expressing cells, rather than from cryptic transactivation of *CYP19A1* because of genomic rearrangements at 15q21.

Acknowledgments This work was supported by the Grant-in-Aid for Scientific Research on Innovative Areas (22132004) from the Ministry of Education, Culture, Sports, Science and Technology, by the Grant-in-Aid for Scientific Research (B) (23390249) from the Japan Society for the Promotion of Science, by the Grant for Research on Intractable Diseases from the Ministry of Health, Labor and Welfare, and by the Grants from National Center for Child Health and Development, from Takeda foundation, and from Daiichi-Sankyo Foundation of Life Science.

Conflict of interest The authors declare that no conflict of interests exists.

References

1. Bulun SE, Lin Z, Imir G, Amin S, Demura M, Yilmaz B, et al. Regulation of aromatase expression in estrogen-responsive breast and uterine disease: from bench to treatment. Pharmacol Rev. 2005;57:359–83.
2. Kulendran M, Salhab M, Mokbel K. Oestrogen-synthesising enzymes and breast cancer. Anticancer Res. 2009;29:1095–109.
3. Bulun SE, Chen D, Lu M, Zhao H, Cheng Y, Demura M, et al. Aromatase excess in cancers of breast, endometrium and ovary. J Steroid Biochem Mol Biol. 2007;106:81–96.
4. Sasano H, Miki Y, Nagasaki S, Suzuki T. In situ estrogen production and its regulation in human breast carcinoma: from endocrinology to intracrinology. Pathol Int. 2009;59:777–89.
5. Bulun SE, Lin Z, Zhao H, Lu M, Amin S, Reierstad S, et al. Regulation of aromatase expression in breast cancer tissue. Ann N Y Acad Sci. 2009;1155:121–31.
6. Demura M, Martin RM, Shozu M, Sebastian S, Takayama K, Hsu WT, et al. Regional rearrangements in chromosome 15q21 cause formation of cryptic promoters for the CYP19 (aromatase) gene. Hum Mol Genet. 2007;16:2529–41.
7. Shozu M, Sebastian S, Takayama K, Hsu WT, Schultz RA, Neely K, et al. Estrogen excess associated with novel gain-of-function mutations affecting the aromatase gene. N Engl J Med. 2003;348:1855–65.
8. Fukami M, Shozu M, Soneda S, Kato F, Inagaki A, Takagi H, et al. Aromatase excess syndrome: identification of cryptic duplications and deletions leading to gain of function of CYP19A1 and assessment of phenotypic determinants. J Clin Endocrinol Metab. 2011;96:E1035–43.
9. Naoi Y, Kishi K, Tanei T, Tsunashima R, Tominaga N, Baba Y, et al. Development of 95-gene classifier as a powerful predictor of recurrences in node-negative and ER-positive breast cancer patients. Breast Cancer Res Treat. 2011;128:633–41.
10. Fridlyand J, Snijders AM, Ylstra B, Li H, Olshen A, Segraves R, et al. Breast tumor copy number aberration phenotypes and genomic instability. BMC Cancer. 2006;6:96.
11. Khan SI, Zhao J, Khan IA, Walker LA, Dasmahapatra AK. Potential utility of natural products as regulators of breast cancer-associated aromatase promoters. Reprod Biol Endocrinol. 2011;9:91.
12. Bulun SE, Price TM, Aitken J, Mahendroo MS, Simpson ER. A link between breast cancer and local estrogen biosynthesis suggested by quantification of breast adipose tissue aromatase cytochrome P450 transcripts using competitive polymerase chain reaction after reverse transcription. J Clin Endocrinol Metab. 1993;77:1622–8.
13. Bulun SE, Simpson ER. Breast cancer and expression of aromatase in breast adipose tissue. Trends Endocrinol Metab. 1994;5:113–20.

Hindawi Publishing Corporation
International Journal of Endocrinology
Volume 2012, Article ID 584807, 8 pages
doi:10.1155/2012/584807

Review Article

Molecular Bases and Phenotypic Determinants of Aromatase Excess Syndrome

Maki Fukami,[1] Makio Shozu,[2] and Tsutomu Ogata[1,3]

[1] *Department of Molecular Endocrinology, National Research Institute for Child Health and Development, 2-10-1 Ohkura, Setagaya, Tokyo 157-8535, Japan*
[2] *Department of Reproductive Medicine, Graduate School of Medicine, Chiba University, 1-8-1 Inohana, Chuo-ku, Chiba City 206-8670, Japan*
[3] *Department of Pediatrics, Hamamatsu University School of Medicine, 1-20-1 Handayama, Higashi-ku, Shizuoka, Hamamatsu 431-3192, Japan*

Correspondence should be addressed to Maki Fukami, mfukami@nch.go.jp

Received 9 July 2011; Revised 22 September 2011; Accepted 2 October 2011

Academic Editor: Rodolfo Rey

Aromatase excess syndrome (AEXS) is a rare autosomal dominant disorder characterized by gynecomastia. This condition is caused by overexpression of *CYP19A1* encoding aromatase, and three types of cryptic genomic rearrangement around *CYP19A1*, that is, duplications, deletions, and inversions, have been identified in AEXS. Duplications appear to have caused *CYP19A1* overexpression because of an increased number of physiological promoters, whereas deletions and inversions would have induced wide *CYP19A1* expression due to the formation of chimeric genes consisting of a noncoding exon(s) of a neighboring gene and *CYP19A1* coding exons. Genotype-phenotype analysis implies that phenotypic severity of AEXS is primarily determined by the expression pattern of *CYP19A1* and the chimeric genes and by the structural property of the fused exons with a promoter function (i.e., the presence or the absence of a natural translation start codon). These results provide novel information about molecular mechanisms of human genetic disorders and biological function of estrogens.

1. Introduction

Aromatase encoded by *CYP19A1* is a cytochrome P450 enzyme that plays a key role in estrogen biosynthesis [1]. It catalyzes the conversion of Δ^4-androstendione into estrone (E_1) and that of testosterone (T) into estradiol (E_2) in the placenta and ovary as well as in other tissues such as the fat, skin, bone, and brain [1].

Overexpression of *CYP19A1* causes a rare autosomal dominant disorder referred to as aromatase excess syndrome (AEXS, OMIM no. 139300) [2–8]. AEXS is characterized by pre- or peripubertal onset gynecomastia, gonadal dysfunction, advanced bone age from childhood to pubertal period, and short adult height in affected males [2–8]. In particular, gynecomastia is a salient feature in AEXS, and, therefore, this condition is also known as hereditary gynecomastia or familial gynecomastia [5]. Affected females may also show several clinical features such as macromastia, precocious puberty, irregular menses, and short adult height [5, 6, 8].

Recently, three types of cryptic genomic rearrangements around *CYP19A1* have been identified in 23 male patients with AEXS [2–4]. The results provide useful implications not only for the clarification of underlying mechanisms but also for the identification of phenotypic determinants. Here, we review the current knowledge about AEXS.

2. The Aromatase Gene (*CYP19A1*)

CYP19A1 encoding aromatase is located on 15q21.2 adjacent to *DMXL2* and *GLDN* (Figure 1) [3, 9]. It spans ~123 kb and consists of at least 11 noncoding exons 1 and nine coding exons 2–10 [9–12]. Each exon 1 is accompanied by a tissue-specific promoter and is spliced alternatively onto a common splice acceptor site at exon 2, although some transcripts are known to contain two of the exons 1 probably due to a splice error [9–11]. Transcription of *CYP19A1* appears to be tightly regulated by alternative usage of the multiple

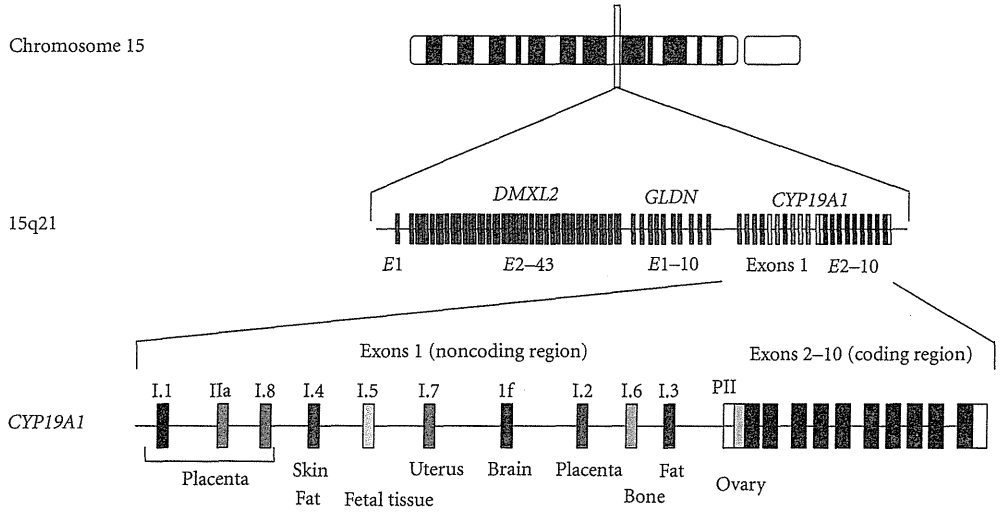

FIGURE 1: Simplified schematic representation indicating the genomic structure of *CYP19A1*. *CYP19A1* is located on 15q21.2 adjacent to *DMXL2* and *GLDN* and consists of at least 11 noncoding exons 1 and nine coding exons 2–10 [9, 10]. Each exon 1 is accompanied by a tissue-specific promoter and is spliced alternatively onto a common splice acceptor site at exon 2 [9–13].

promoters [9–13]. Actually, *CYP19A1* is strongly expressed in the placenta and moderately expressed in the ovary, whereas it is only weakly expressed in a rather limited number of tissues including skin, fat, and hypothalamus [4, 13]. Of the 11 noncoding exons 1, exon I.4 seems to play a critical role in the regulation of estrogen biosynthesis in males, because this exon contains the major promoter for extragonadal tissues [9, 10].

3. Molecular Bases of AEXS

A family with dominantly transmitted gynecomastia of prepubertal onset was first described in 1962 by Wallach and Garcia [14]. After this initial report, several cases have been described [5–8, 15]. Laboratory examinations of the affected males revealed markedly elevated serum estrogen values and estrogen/androgen ratios and significantly increased aromatase activity in fibroblasts and lymphocytes [5–8, 15]. Linkage analyses in two families indicated a close association between *CYP19A1*-flanking polymorphic markers and the disease phenotype [5, 6]. Thus, the condition was assumed to be caused by gain-of-function mutations of *CYP19A1*, and, therefore, the name of AEXS was coined for this condition [7, 8]. However, since direct sequencing and Southern blotting analysis failed to detect mutations or copy number abnormalities in the coding region of *CYP19A1* [5, 6], the molecular basis of this entity remained elusive until recently.

In 2003, Shozu et al. reported a father-son pair and a sporadic case with AEXS in whom they identified heterozygous chromosomal inversions of the chromosome 15 [2]. Subsequently, Demura et al. performed detailed molecular studies for these cases and additional two cases and characterized four types of inversions affecting the 5′ region of *CYP19A1* [3]. Each inversion has resulted in the formation of a chimeric gene consisting of *CYP19A1* coding exons and exon 1 of the widely expressed neighboring genes, that is, *CGNL1*, *TMOD3*, *MAPK6*, and *TLN2*. These data imply that overexpression of *CYP19A1* in the inversion-positive cases are caused by cryptic usage of constitutively active promoters. Consistent with this, *in silico* analysis revealed the presence of promoter-compatible sequences around exon 1 of *CGN1*, *TMOD3*, and *MAPK6* in multiple cell types, although such sequences remain to be identified for noncoding exons of *TLN2* [4].

We recently studied 18 males from six families with AEXS (families A–F) and identified three types of heterozygous cryptic genomic rearrangements in the upstream region of the *CYP19A1* coding exons (Figure 2) [4]. In families A and B, we identified the same 79,156 bp tandem duplication encompassing seven of the 11 noncoding exons 1 of *CYP19A1*. Notably, this duplication includes exon I.4 that functions as a major promoter for extragonadal tissues such as fat and skin; therefore, *CYP19A1* overexpression in these families would be explained by increasing the number of this promoter. Indeed, RT-PCR analysis detected a splice variant consisting of exon I.4 at the 5′ side and exon I.8 at the 3′ side in lymphoblastoid cell lines and skin fibroblasts of the patients, indicating that the duplicated exon I.4 at the distal nonphysiological position actually functions as transcription start sites. In family C, we identified a 211,631 bp deletion affecting exons 2–43 of *DMXL2* and exons 5–10 of *GLDN*. This deletion appears to have caused *CYP19A1* overexpression because of cryptic usage of *DMXL2* exon 1 as an extra transcription start site for *CYP19A1*. Indeed, RT-PCR revealed the presence of chimeric mRNA clones consisting of *DMXL2* exon 1 and *CYP19A1* exon 2, supporting the notion that aberrant splicing has occurred between these two exons. Such *DMXL2/CYP19A1* chimeric mRNA accounted for 2–5% of *CYP19A1*-containing transcripts from skin fibroblasts. In families D–F, we identified

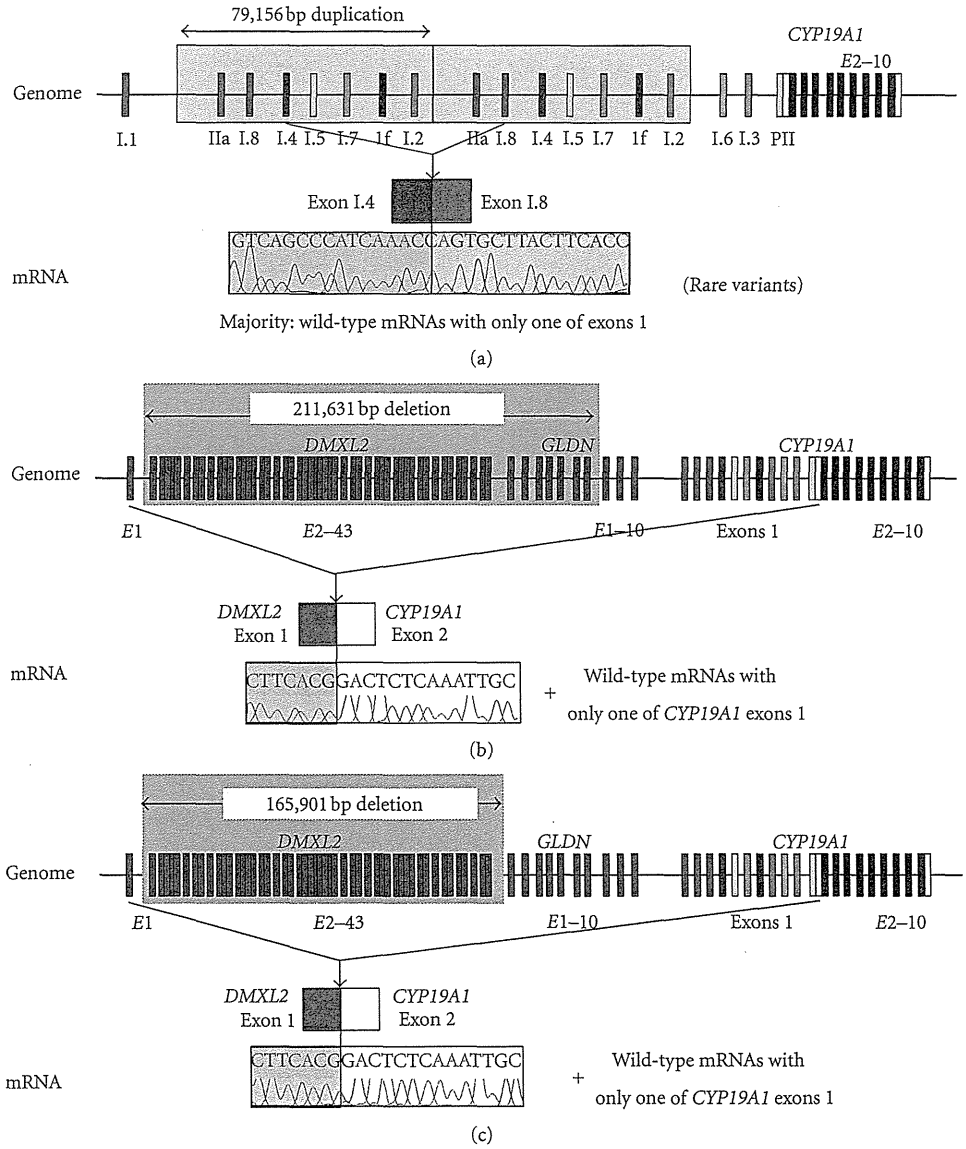

FIGURE 2: Schematic representation of duplications and deletions identified in patients with AEXS. (a) the tandem duplication of families A and B [4]. Genome: the duplication (yellow boxes) includes seven of the 11 noncoding exons 1 of *CYP19A1*. mRNA: the sequence of a rare transcript is shown. The 3′-end of exon I.4 is connected with the 5′-end of exon I.8. (b) The deletion of family C [4]. Genome: the deletion (a gray area) includes exons 2–43 of *DMXL2* and exons 5–10 of *GLDN*. mRNA: The sequence of a rare chimeric gene transcript is shown. *DMXL2* exon 1 consisting of a noncoding region and a coding region is spliced onto the common acceptor site of *CYP19A1* exon 2. (c) The deletion of families D–F [4]. Genome: the deletion (a gray area) includes exons 2–43 of *DMXL2*. mRNA: the sequence of a rare chimeric gene transcript is delineated. The mRNA structure is the same as that detected in family C.

an identical 165,901 bp deletion including exons 2–43 of *DMXL2*. RT-PCR identified the same chimeric mRNA as that detected in family C.

Collectively, three types of genomic rearrangements on 15q21 have been identified in AEXS to date, namely, inversion type (four subtypes), duplication type, and deletion type (two subtypes) (Figure 3(a)) [2–4]. In this regard, sequence analyses for the breakpoints have indicated that (1) inversion types are formed by a repeat sequence-mediated nonallelic intrachromosomal or interchromosomal recombination or by a replication-based mechanism of fork stalling and template switching (FoSTeS) that occurs in the absence of repeat sequences and is often associated with microhomology [16], (2) duplication type is generated by FoSTeS, and (3) deletions are produced by nonhomologous end joining that takes place between nonhomologous sequences and is frequently accompanied by an insertion of a short segment at the fusion point or by a nonallelic recombination [16].

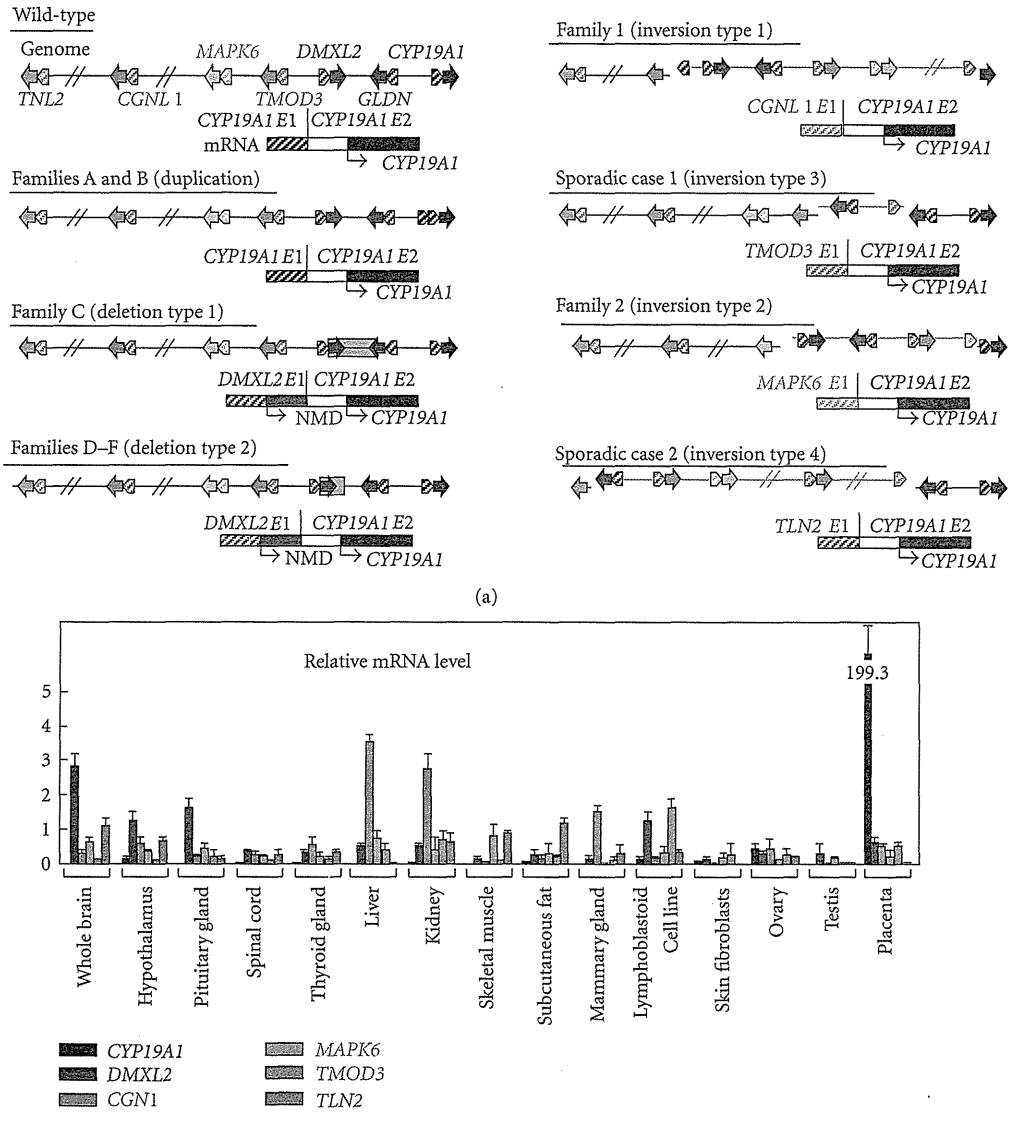

FIGURE 3: Structural and functional properties of the fused exons. (a) Schematic representation of the rearranged genome and mRNA structures. The white and the black boxes of *CYP19A1* exon 2 show untranslated region and coding region, respectively. For genome, the striped and the painted arrows indicate noncoding and coding exons, respectively (5′ → 3′). The inverted genomic regions are delineated in blue lines. For mRNA, colored striped boxes represent noncoding regions of each gene. The *DMXL2-CYP19A1* chimeric mRNA has two translation initiation codons and therefore is destined to produce not only *CYP19A1* protein but also a 47 amino acid protein which is predicted to undergo nonsense-mediated mRNA decay (NMD). The deletion and the inversion types are associated with heterozygous impairment of neighboring genes (deletion or disconnection between noncoding exon(s) and the following coding exons). The inversion subtype 1 is accompanied by inversion of eight of the 11 *CYP19A1* exons 1, and the inversion subtype 2 is associated with inversion of the placenta-specific *CYP19A1* exon I.1. (b) Expression patterns of *CYP19A1* and the five neighboring genes involved in the chimeric gene formation [4]. Relative mRNA levels against *TBP* in normal human tissues are shown.

Thus, it appears that genomic sequence around *CYP19A1* harbors particular motifs that are vulnerable to replication- and recombination-mediated errors. The results provide novel mechanisms of gain-of-function mutations leading to human diseases.

4. Clinical Features of AEXS

To date, a total of 23 male cases from 10 families have been reported to have molecularly confirmed AEXS (Table 1, Figure 3(a)) [2–4]. They exhibited pre- or peripubertal onset

Table 1: Summary of clinical studies in male patients with aromatase excess syndrome (modified from [4]).

(a)

Family			Family A			Family B		Family C				Family D			Family E	
Mutation types			Duplication			Duplication		Deletion				Deletion			Deletion	
The promoter involved in *CYP19A1* overexpression			*CYP19A1*			*CYP19A1*		*CYP19A1*				*DMXL2*			*DMXL2*	
Case		Case 1	Case 2		Case 3	Case 4		Case 5		Case 6		Case 7	Case 8		Case 9		Case 10	
Age at examination (year)		66	15		20	15		15		13		42	9		12		13	
<Phenotypic findings>																		
Gynecomastia (tanner breast stage)		**2**	**2**		**2**	**3**		**4**		**4**		**4**	**3**		**4**		**4**	
Onset of gynecomastia (year)		**13**	**13**		**10**	**11**		**12**		**11**		**11**	**7**		**9**		**10**	
Mastectomy (year)		No	**Yes (15)**		No	**Yes (15)**		**Yes (15)**		**Yes (13)**		No	No		**Yes (12)**		**Yes (13)**	
Testis (ml)		N.E.	**12**		**12**	**12**		**12**		12		N.E.	3		12		20	
Pubic hair (tanner stage)		N.E.	2-3		4	5		4		3		N.E.	1		3		4	
Facial hair		Normal	Scarce		**Scarce**	Normal		Absent		Absent		N.E.	Absent		Absent		Absent	
Height (SDS)[a]		−1.2	−0.3		+0.4	+0.8		−2.0		−1.0		−1.6	**+2.7**		±0		+1.8	
Bone age (year)[b]		N.E.	N.E.		N.E.	16.0		16.0		13.5		N.E.	**13.0**		**15.0**		**17.0**	
Fertility (spermatogenesis)		Yes	?		(Yes)[h]	?		?		?		Yes	?		?		?	
<Endocrine findings>[c]		B	B	S	B	S	B	S	B	S	B	S	B	B	S	B	S	B	S
<At Dx>	Stimulus																		
LH (mIU/mL)	GnRH[e]	3.8	2.3	**14.3**	2.1	**17.0**	2.4	29.4	1.9	40.6	1.8	69.2		1.1	11.5	**0.6**	39.5	6.7	14.8
LH (mIU/mL)	GnRH (after priming)[f]		1.8	**9.5**	**1.3**	**10.7**													
FSH (mIU/mL)	GnRH[e]	**1.7**	**3.1**	**5.3**	**<0.5**	**1.2**	**0.9**	**2.4**	**1.4**	**4.2**	**2.0**	**7.8**		**3.2**	**6.6**	**0.6**	**2.9**	**0.7**	**1.0**
FSH (mIU/mL)	GnRH (after priming)[f]		**2.6**	**3.2**	**<0.5**	**0.9**													
Prolactin (ng/ml)			4.3		5.3				8.2		9.1			11.3		18.8			
Δ^4A (ng/mL)		**0.5**			**1.1**		**1.2**						**0.6**			**0.7**		**2.4**	2.9
T (ng/mL)	hCG[g]	2.9	**1.6**		**2.2**		4.0		**2.6**	7.2	**1.4**	7.9		**0.6**	3.6	**2.4**		3.2	9.7
DHT (ng/mL)		0.4			0.2													0.4	1.2
Inhibin B (pg/mL)		**61.6**			**74.6**		**83.5**		**75.2**										
E_1 (pg/mL)		157			120		124						57			63		53	
E_2 (pg/mL)		29	15		22		59		56		38		24	19		25		58	
E_2/T ratio ($\times 10^3$)		10.0	9.4		10.0		14.8		21.5		27.1			31.7		10.4		18.1	

(b)

Family		Family F								Family G		Family H		Sporadic	
Mutation types		Deletion								Inversion		Inversion		Inversion	
The promoter involved in *CYP19A1* overexpression		*DMXL2*								*CGNL1*		*MAPK6*		*TMOD3*	*TLN2*
Case		Case 11	Case 12	Case 13	Case 14	Case 15	Case 16	Case 17	Case 18	Case 19	Case 20	Case 21[j]		Case 22	Case 23
Age at examination (year)		69	35	44	45	9	8	13	10	35	7	13		17	36
<Phenotypic findings>															
Gynecomastia (tanner breast stage)		**Yes**[i]	**Yes**[i]	**Yes**[i]	**Yes**[i]	**2**	**3**	**3**	**3**	**Yes**	**3**	**5**		N.E.	**Yes**
Onset of gynecomastia (year)		?	?	?	?	**8**	**8**	**11**	**10**	**5**	**5**	**8**		**7**	?
Mastectomy (year)		**Yes**[i]	**Yes**[i]	**Yes**[i]	**Yes**[i]	No	No	**Yes (?)**	**Yes (?)**	**Yes (16)**	No	**Yes (?)**		**Yes (?)**	**Yes (19)**
Testis (ml)		N.E.	N.E.	N.E.	N.E.	2	1.5	**2**	2	N.E.	N.E.	N.E.		Normal	N.E.
Pubic hair (tanner stage)		N.E.	N.E.	N.E.	N.E.	1	1	2	1	Normal	1	**2-3** (at 21.0)		N.E.	N.E.
Facial hair		N.E.	N.E.	N.E.	N.E.	Absent	Absent	Absent	Absent	**Absent**	Absent	N.E.		**Scarce**	N.E.
Height (SDS)[a]		N.E.	~ −1.5	~ −1.5	~ −1.5	+1.4	N.E.	**+2.0**	**+2.4**	**Short**	**>+2.5**	−1.6 (at 21.0)		**Short**	N.E.
Bone age (year)[b]		N.E.	N.E.	N.E.	N.E.	**12.5**	**13.0**	**15.0**	**14.5 (at 12.5)**	N.E.	**13.0 (at 5.5)**	**17.0**		N.E.	N.E.
Fertility (spermatogenesis)		Yes	Yes	Yes	Yes	?	?	?	?	Yes	?	?		?	?
<Endocrine findings>[c]		B	B	B	B	B	B	B S	B	B	B	B	S	B	
<At Dx>	Stimulus														
LH (mIU/mL)	GnRH[e]	**0.2**	3.5	1.7	3.0	0.2	<0.1	2.6 6.3	1.5	1.7	0.1	2.6	**10.0**	4.3	
LH (mIU/mL)	GnRH (after priming)[f]														
FSH (mIU/mL)	GnRH[e]	**1.4**	**2.3**	**0.8**	**0.8**	1.4	0.5	**0.8 1.2**	**1.2**	**1.5**	0.3	**<0.1**	**<0.1**	**2.7**	
FSH (mIU/mL)	GnRH (after priming)[f]														
Prolactin (ng/ml)															
Δ^4A (ng/mL)		1.4	**0.4**	1.7	**0.5**	0.3	<0.3	**0.9** 1.5	1.3	**0.8**	0.3	2.4	**0.9**		
T (ng/mL)	hCG[g]	**2.6**	**2.5**	**2.1**	**2.5**	<0.1	<0.1	**2.7** 9.2	**2.7**	3.2	<0.1	**1.2**	3.8	**2.3**	
DHT (ng/mL)												0.2	0.5		
Inhibin B (pg/mL)															
E_1 (pg/mL)		32	34	59	34	26	41	77	86	903	119	544		556	
E_2 (pg/mL)		10	19	24	31	11	7	25	40	223	15	178		392	
E_2/T ratio ($\times 10^3$)		3.8	7.6	11.4	12.4			9.3	14.8	69.6		148.3		170.4	

SDS: standard deviation score; Dx: diagnosis; Tx: therapy; LH: luteinizing hormone; FSH: follicle stimulating hormone; Δ^4A: androstenedione; T: testosterone; DHT: dihydrotestosterone; E_1: estrone; E_2: estradiol; GnRH: gonadotropin-releasing hormone; hCG: human chorionic gonadotropin; N.E.: not examined; B: basal; and S: stimulated.

Abnormal clinical findings are boldfaced.

Abnormally low hormone values are boldfaced, and abnormally high hormone values are underlined.

[a]Evaluated by age- and ethnicity-matched growth references; heights ≥+2.0 SD or below ≤ −2.0 SD were regarded as abnormal.

[b]Assessed by the Tanner-Whitehouse 2 method standardized for Japanese or by the Greulich-Pyle method for Caucasians; bone age was assessed as advanced when it was accelerated a year or more.

[c]Evaluated by age-matched male reference data, except for inhibin B and E_1 that have been compared with data from 19 adult males.

[d]Treated with aromatase inhibitors (anastrozole).

[e]GnRH 100 μg/m^2 (max. 100 μg) bolus i.v.; blood sampling at 0, 30, 60, 90, and 120 minutes.

[f]GnRH test after priming with GnRH 100 μg i.m. for 5 consecutive days.

[g]hCG 3000 IU/m^2 (max 5000 IU) i.m. for 3 consecutive days; blood sampling on days 1 and 4.

[h]Although Case 3 has not yet fathered a child, he has normal spermatogenesis with semen volume of 2.5 ml (reference value: >2 ml), sperm count of 105 × 10^6/ml (>20 × 10^6/ml), total sperm count of 262.5 × 10^6 (>40 × 10^6), motile cells of 70% (>50%), and normal morphological sperms 77% (>30%).

[i]These four patients allegedly had gynecomastia that required mastectomy (age unknown).

[j]The sister has macromastia, large uterus, and irregular menses; the parental phenotype has not been described.

The conversion factor to the SI unit: LH 1.0 (IU/L), FSH 1.0 (IU/L), E_1 3.699 (pmol/L), E_2 3.671 (pmol/L), Δ^4A 3.492 (nmol/L), and T 3.467 (nmol/L).

gynecomastia, small testes with fairly preserved masculinization, obvious or relative tall stature in childhood and grossly normal or apparent short stature in adulthood, and age-appropriate or variably advanced bone ages. Blood endocrine studies revealed markedly elevated E_1 values and E_2/T ratios in all cases examined and normal or variably elevated E_2 values. In addition, Δ^4-androstenedione, T, and dihydrotestosterone values were low or normal, and human chorionic gonadotropin (hCG) test indicated normal T responses. Notably, LH values were grossly normal at the baseline and variably responded to GnRH stimulation, whereas FSH values were low at the baseline and poorly responded to GnRH stimulation even after preceding GnRH priming, in all cases examined.

The severity of such clinical phenotypes is primarily dependent on the underlying mechanisms (Table 1). They are obviously mild in the duplication type, moderate in the deletion type, and severe in the inversion type, except for serum FSH values that remain suppressed irrespective of the underlying mechanisms. Likewise, gynecomastia has been reported to be ameliorated with 1 mg/day of aromatase inhibitor (anastrozole) in the duplication and the deletion types and with 2–4 mg/day of anastrozole in the inversion type [4].

5. Expression Pattern of *CYP19A1* and the Chimeric Genes as One Phenotypic Determinant

Phenotypic severity is much milder in the duplication type than in the deletion and the inversion types. This would be explained by the tissue expression pattern of *CYP19A1* and the chimeric genes. Indeed, RT-PCR analysis using normal human tissue samples revealed that *CYP19A1* is expressed only in a limited number of tissues such as placenta, ovary, skin, and fat, while the five genes involved in the formation of chimeric genes are widely expressed with some degree of variation (Figure 3(b)). Therefore, it is likely that the duplication types would simply increase *CYP19A1* transcription in native *CYP19A1*-expressing tissues, whereas the deletion and the inversion types lead to *CYP19A1* overexpression in a range of tissues, because expression patterns of chimeric genes are predicted to follow those of the original genes. Furthermore, it is also likely that the native *CYP19A1* promoter is subject to negative feedback by elevated estrogens [17], whereas such negative feedback effect by estrogen is weak or even absent for the chimeric genes in the deletion and the inversion types.

6. Structural Property of the Fused Exons as Another Phenotypic Determinant

Phenotypic severity is also milder in the deletion type than in the inversion types, despite a similar wide expression pattern of genes involved in the chimeric gene formation (Table 1, Figure 3(b)). In this context, it is noteworthy that a translation start codon and a following coding region are present on exon 1 of *DMXL2* of the deletion type but not on exons 1 of the chimeric genes of the inversion types (Figure 3(a)). Thus, it is likely that *DMXL2/CYP19A1* chimeric mRNAs transcribed by the *DMXL2* promoter preferentially recognize the natural start codon on *DMXL2* exon 1 and undergo nonsense-mediated mRNA decay and that rather exceptional chimeric mRNAs, which recognize the start codon on *CYP19A1* exon 2, are transcribed into CYP19A1 protein. By contrast, such a phenomenon would not be postulated for the inversion-mediated chimeric mRNAs. Consistent with this, it has been shown that the *DMXL2/CYP19A1* chimeric mRNA is present only in 2–5% of *CYP19A1*-containing transcripts from skin fibroblasts, whereas the *CGNL1/CYP19A1* chimeric mRNA and the *TMOD3/CYP19A1* chimeric mRNA account for 89–100% and 80% of transcripts from skin fibroblasts, respectively [2, 4].

In addition, the genomic structure caused by the rearrangements would affect efficiency of splicing between noncoding exon(s) of neighboring genes and *CYP19A1* exon 2. For example, in the inversion subtype 1, the physical distance between *CGNL1* exon 1 and *CYP19A1* exon 2 is short, and, while a splice competition may be possible between exon 1 of neighboring genes and original *CYP19A1* exons 1, eight of 11 *CYP19A1* exons 1 including exon I.4 have been disconnected from *CYP19A1* coding exons by inversion (Figure 3(a)). This may also enhance the splicing efficiency between *CGNL1* exon 1 and *CYP19A1* exon 2 and thereby lead to relatively severe overexpression of the *CGNL1-CYP19A1* chimeric gene, although this hypothesis would not be applicable for other chimeric genes.

7. Implication for the Hypothalamus-Pituitary-Gonadal Axis Function

It is notable that a similar degree of FSH-dominant hypogonadotropic hypogonadism is observed in the three types, although E_1 and E_2 values and E_2/T ratios are much higher in the inversion type than in the duplication and deletion types (Table 1). In particular, FSH was severely suppressed even after GnRH priming in the duplication type [4]. This implies that a relatively mild excess of circulatory estrogens can exert a strong negative feedback effect on FSH secretion primarily at the pituitary. This would be consistent with the results of animal studies that show strong inhibitory effect of E_2 on transcription of FSH beta-subunit gene in the pituitary cells and almost negligible effect on synthesis of LH beta-subunit and secretion of LH [18, 19]. In this regard, while T responses to hCG stimulation are normal in the duplication and the deletion types and somewhat low in the inversion type, this would be consistent with fairly preserved LH secretion in the three types and markedly increased estrogen values in the inversion type. In addition, whereas fertility and spermatogenesis are normally preserved in the three types, this would be explained by the FSH-dominant hypogonadotropic hypogonadism, because FSH plays only a minor role in male fertility (spermatogenesis) [20].